Polymer Degradation and Stability 185 (2021) 109497

Contents lists available at ScienceDirect

Polymer Degradation and Stability

journal homepage: www.elsevier.com/locate/polymdegradstab

# Prevention of the formation of respirable fibers in carbon fiber reinforced epoxy resins during combustion by phosphorus or silicon containing flame retardants

Lara Greiner[a,b,*], Manfred Döring[b], Sebastian Eibl[a]

[a] Bundeswehr Research Institute for Materials, Fuels and Lubricants, Institutsweg 1, 85435 Erding, Germany
[b] Fraunhofer Institute for Structural Durability and System Reliability LBF, Schlossgartenstr. 6, 64289 Darmstadt, Germany

ARTICLE INFO

*Article history:*
Received 30 September 2020
Revised 1 January 2021
Accepted 19 January 2021
Available online 21 January 2021

*Keywords:*
Carbon fiber reinforced epoxy resin
Fiber fragments
Fiber protecting mechanism
Phosphorus containing flame retardant

ABSTRACT

The influence of different phosphorus containing flame retardants on fiber degradation during combustion of carbon fiber reinforced epoxy resins is described. A phosphazene, a phosphate and a phosphinate were investigated in HexFlow® RTM6, a high performance epoxy resin designed for resin transfer moulding processes, and composites thereof. UL94-V flammability tests of neat RTM6 samples showed a high flame retardant efficiency of the phosphate and the phosphazene. The burning behavior of carbon fiber reinforced composite samples with various amounts of flame retardants was investigated by cone calorimetry and the influence on fiber degradation was determined by scanning electron microscopy including energy dispersive X-ray spectroscopy. While phosphazene acting mainly in the gas phase showed the best flame retardant efficiency in the composite, the phosphate acting mainly in the condensed phase showed the best fiber protection. Mechanical properties were not affected significantly by the incorporation of flame retardants ensuring the application in components manufactured by resin transfer moulding. Finally combinations of phosphazene and a silicon compound were tested. No synergism regarding fiber protection or flame retardancy was observed in carbon fiber reinforced epoxy resins, but these investigations provide information about efficient fiber protection mechanisms.



## 1. Introduction

Carbon fiber reinforced polymer (CFRP) composites are widely used in aircraft and automotive construction as lightweight materials with optimized mechanical properties. Especially epoxy-based composites can be found in numerous high sophisticated space and aerospace applications, mainly in structural components. For many applications, adjusted flame retardancy is necessary. Since the neat epoxy resin sets a base value for the burning behavior of a material, the efficiency of incorporated flame retardants depends on the epoxy resin matrix and the reinforcement [1–7]. Additionally, several aircraft crashes accompanied by fire have increased the interest in assessing an additional health risk due to the formation of respirable carbon fiber dust. Critical fiber concentrations were reported for large scale fire tests as well as a helicopter crash while collecting the flight recorder [8,9]. It is well known that carbon fibers can form respirable fiber fragments after thermal load and fire [10,11]. All types of carbon fibers consist of more than 90% carbon (typically over 95%) and apart from that of mainly nitrogen, which makes them prone to oxidation reaction. A significant oxidation reaction is observed above 600 °C in air within minutes, slightly influenced by heating rate and strongly influenced by oxygen concentration [12]. Thermo-oxidative degradation is expressed in principal by two phenomena: a continuous decrease of fiber diameter and the formation of surface defects, which end up in a pronounced hole structure at severe damage. Fibers thinner than 3 µm were observed for example after 10 min at 650 °C [12]. According to the definition of the World Health Organization (WHO), fibers are considered to be respirable, if they are thinner than 3 µm and longer than 5 µm. Fibers with this dimensions are thin enough to penetrate the deep lung areas (alveola), and too long to be easily exhaled [13]. Additionally, the length to diameter ratio has to be higher than 3. Commercially available carbon fibers are typically thicker than 5 µm and therefore uncritical with respect to inhalation, as long as CFRP material has not undergone high temperatures during fire or other degradation processes. On the side of passive measures of fire protection, it is necessary to improve the thermal properties of composites with respect to the release of respirable fibers during or

* Correspondence author.
*E-mail address:* LaraGreiner@bundeswehr.org (L. Greiner).

https://doi.org/10.1016/j.polymdegradstab.2021.109497
0141-3910/

after a fire. A strategy that does not affect the fiber to matrix adhesion is to add a flame retardant to the resin matrix, which forms a protection layer on the fiber surface during combustion [14]. Zinc borate was used successfully but it is not suitable for resin transfer moulding, an important process for the manufacturing of fiber-reinforced epoxy based composites. It increases the viscosity of the resin significantly and the inhomogeneously dispersed particles are filtered by the fiber plies during injection. Therefore a suitable flame retardant, that is soluble in the epoxy resin matrix and protects the fiber, has to be found. Phosphorus containing flame retardants offer a halogen-free way to render epoxy resins and their composites flame retardant. For phosphorus containing flame retardants, the mode of action depends on the phosphorus species and the polymer they are incorporated [15,16]. The chemical environment of phosphorus can either be carbon / hydrogen rich and promote action in the gas phase or it can be oxygen rich and promote action in the condensed phase. Furthermore, a trend to apply polymeric or oligomeric flame retardants is observed to avoid leaching. For these investigations three different phosphorus containing flame retardants were incorporated: An oligomeric/cyclic resorcinol bis(diphenyl phosphate) most likely to act in the condensed phase by the formation of polyphosphoric acid ([17,18] a condensed polymeric adduct of 9,10-dihydro-9-oxa-10-phosphaphenanthrene-10-oxide (DOPO) and salicylaldehyde, as well as bis(phenoxy)phosphazene that may act in the gas phase or in the condensed phase depending on the matrix [19]. The goal of this investigation is to determine, if phosphorus containing flame retardants can be used for fiber protection as well and if there is a correlation between the flame retardant mode of action and the influence on the fiber degradation. Another approach in flame retardancy of epoxy resins is the use of silicon compounds [20,21] and especially the interplay of phosphorus and silicon compounds [22-25]. There are both, synergistic [26-28] and antagonistic [24], effects reported. Therefore, and because of possible barrier properties of silicon dioxide, nanoscale silicon dioxide particles diluted in bisphenol A diglycidylether (DGEBA), suitable for resin transfer moulding processes were tested as well. These studies provide information on the fiber protection mechanism.

## 2. Experimental

### 2.1. Material

Reaction-to-fire tests were performed with the carbon fiber reinforced system HexFlow® RTM6 (epoxy resin matrix based on tetraglycidyl methylene dianiline and aromatic aminic hardeners) and HexForce® G0939 (carbon fiber fabric) from Hexcel Composites GmbH (Stade, Germany) [29]. The matrix was modified by adding an oligomeric bis(phenoxy)phosphazene (SPB®100, Hebron S.A., "SPB100") or a condensed adduct of 9,10-dihydro-9-oxa-10-phosphaphenanthrene-10-oxide and salicylaldehyde (HFC-X®, DIC Corporation, "HFC-X") or an oligomeric resorcinol bis(diphenyl phosphate) (Aflammit®PLF280, THOR Group Ltd., "RDP") in different quantities up to 15% related to the resin mass. For modifications with silicon compounds, silicon dioxide nanoparticles with a diameter of 20 nm homogeneously dispersed in Bisphenol A diglycidyl ether was used (Nanopox® F400, 40 wt% $SiO_2$, Evonik, Germany, "NPF400"). The different formulations were mixed at 120 °C for 15 min. 8 or 16 piles were laminated by hand resulting in 2 or 4 mm thick lay-ups: $[(0|90)]_8$ and $[(0|90)]_{16}$. This procedure is described in the literature [30]. Specimens were cured in an autoclave according to the manufacturer's recommended conditions [29]. The cured laminates were cut with a water-cooled diamond wheel saw into specimens of 100 mm x 100 mm for cone calorimetric measurements and specimens of 20 mm x 10 mm for the measurement of the interlaminar shear strength. Additionally samples of flame retarded RTM6 without fiber reinforcement were prepared (2 mm, 4 mm). Curing of these samples was carried out with the same temperature program but under atmospheric pressure. Specimens of 30 mm x 10 mm x 2 mm for dynamic mechanical analysis and 70 mm x 13 mm x 4 mm for UL94-tests were trimmed with a band-saw. An overview of the prepared samples is given in Table 1. Chemical structures of the phosphorus containing flame retardants are shown in Fig. 1.

**Table 1**
Prepared samples based on RTM6 resin.

| Flame Retardant in RTM6-Matrix | Reinforcement | *Thickness* / mm |
|---|---|---|
| - | - \| CF | 2 \| 4 |
| 4% SPB100 | CF | 2 |
| 10% SPB100 | - \| CF | 2 \| 4 |
| 15% SPB100 | CF | 2 |
| 5% RDP | CF | 2 |
| 10% RDP | - \| CF | 2 \| 4 |
| 5% HFC-X | CF | 2 |
| 10% HFC-X | - \| CF | 2 \| 4 |
| 10% NPF400 | CF | 2 |
| 5% SPB100 + 5% NPF400 | CF | 2 |
| 7% SPB100 + 3% NPF400 | CF | 2 |

CF: Carbon Fiber.
-: no reinforcement.

### 2.2. Characterization

4 mm thick specimens were analyzed by UL-94 (Dr.-Ing. Georg Wazau Mess- + Prüfsysteme GmbH, Germany) according to DIN EN 60,695–11–10 [31] and 2 mm thick specimens were investigated by dynamic mechanical analysis (DMA; SEIKO SII EXSTAR 6100 DMS, Seiko Instruments Inc, Japan) with single cantilever geometry from 35 °C to 260 °C with a frequency of 1 Hz and a heating rate of 3 $K \cdot min^{-1}$. Thermogravimetric analyses (TGA; Q500, TA Instruments, Inc., USA) of the compact material were performed starting at room temperature and heated to 800 °C in nitrogen or synthetic air (50 ml/min) with a heating rate of 10 $K \cdot min^{-1}$. Cone calorimetric measurements (Fire Testing Technology Ltd, England) of fiber-reinforced specimens were carried out in order to determine reaction-to-fire characteristics such as heat release, mass loss, formation of smoke etc. [32] according to ISO 5660 [33] in non-scrubbed mode. Specimens (100 × 100 mm [2] were wrapped in aluminum foil at the backside, supported on mineral wool, inserted in a frame sample holder, and irradiated at a heat flux of 60 $kW \cdot m^{-2}$ for reinforced samples and at a heat flux of 35 $kW \cdot m^{-2}$ for neat resin samples. 60 $kW \cdot m^{-2}$ correspond more to fully developed fires and are used to observe the fiber degradation while 35 $kW \cdot m^{-2}$ correspond to developing fires [34]. Test duration (5 min, 10 min, 20 min, 25 min) and sample thickness (2 mm, 4 mm) were varied for further investigations. Temperature rises were recorded by thermocouples (type K) attached to the middle of the front side of the specimens by a high-temperature resistant tape. This tape burns simultaneously to the resin matrix but leaves the thermocouple touching the sample surface for the rest of the measurement. The thermocouples were located close to the center of each panel. A scanning electron microscope (SM-300, TOPCON Corp.) was used for the determination of fiber diameters. For each given value, the diameters of at least 30 fibers are averaged. EDX analyses were done with an EVO HD 25 (Carl Zeiss Microscopy GmbH, 5 kV) scanning electron microscope. Interlaminar shear strength (ILSS) tests were performed for 2 mm thick specimens in accordance to EN 2563 by a three-point flexural test with a universal mechanical testing machine (Z020, ZwickRoell GmbH & Co. KG, Germany) [35]. Rheological measurements in dependence on temperature (dynamic) and time (isothermal) were carried out with a rotational rheometer HAAKE MARS I (ThermoFischer Sci-

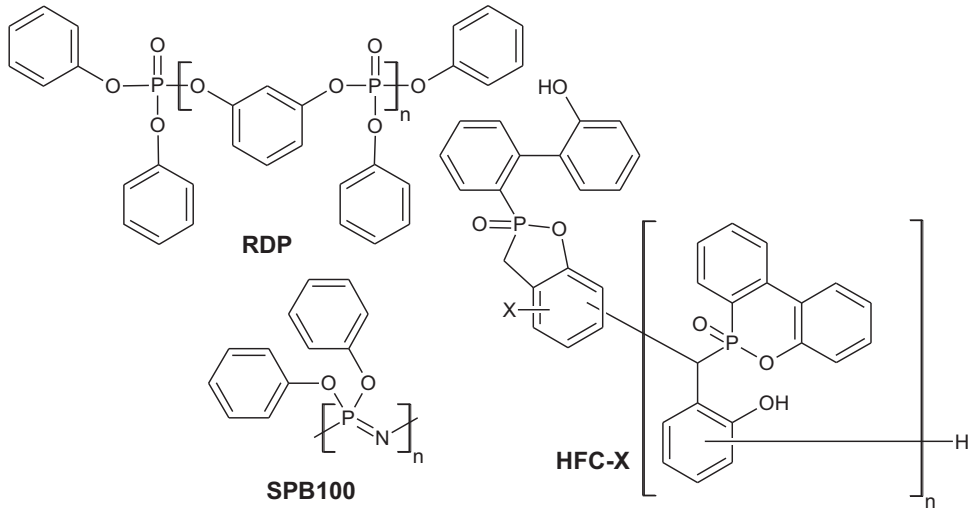


**Fig. 1.** Chemical structures of phosphorus containing flame retardants used in this investigation.

**Table 2**
Glass transition temperatures and moisture uptake of RTM6 samples.

| Sample | $T_g$(Max(tan(δ))) / °C | Moisture uptake / % | $T_{g,wet}$(Max(tan(δ))) / °C |
|---|---|---|---|
| **RTM6** | 215 | 2 | 218 |
| + 10% RDP | 190 | 2 | 190 |
| + 10% SPB100 | 199 | 2 | 199 |
| + 10% HFC-X | 205 | 2 | 207 |

**Table 3**
$T_{max}$, $T_{1\%}$, $T_{5\%}$ and residue of formulations of RTM6 and phosphorus containing flame retardants obtained by TG measurements in air or nitrogen atmosphere with a heating rate of 10 K·min$^{-1}$.

| Sample | $T_{max}$ / °C | $T_{1\%}$ / °C | $T_{5\%}$ / °C | Residue / % |
|---|---|---|---|---|
| **RTM6 in $N_2$** | 379 | 265 | 341 | 9 (800 °C) |
| + 10% RDP | 346 | 240 | 297 | 23 (800 °C) |
| + 10% SPB100 | 379 | 254 | 323 | 15 (800 °C) |
| + 10% HFC-X | 345 | 261 | 307 | 20 (800 °C) |
| **RTM6 in *air*** | I 369 \| II 572 | 229 | 331 | 33 (492 °C) \| 0 (800 °C) |
| + 10% RDP | I 350 \| II 555 | 232 | 292 | 53 (416 °C) \| 3 (800 °C) |
| + 10% SPB100 | I 377 \| II 543 | 264 | 325 | 39 (465 °C) \| 3 (800 °C) |
| + 10% HFC-X | I 365 \| II 545 | 237 | 309 | 49 (432 °C) \| 2 (800 °C) |

entific, Massachusetts, USA). A plate-plate measurement geometry in oscillation mode was chosen. The gap between the plates was 0.5 mm and the frequency 1 s$^{-1}$. The heating rate was 1 K·min$^{-1}$ for dynamic measurements.

## 3. Results and discussion

### 3.1. Material characterization

Glass transition temperatures were determined by dynamic mechanical analysis (DMA) as the temperature corresponding to the maximum of the dissipation factor tan$(\delta)$ denoted by $T_g$(Max(tan(δ))). The results are shown in Table 2. RDP lowers the glass transition temperature by 25 °C compared to the pure resin. Since RDP is the only liquid flame retardant and has the lowest molecular mass and weakest intermolecular interactions, it reduces glass transition temperature the most compared to SPB 100 and HFC-X. SPB100 lowers the glass transition temperature by 16 °C and HFC-X by 10 °C, meaning a negligible change of the glass transition temperature according to literature [1,36]. The phenolic OH-groups of HFC-X react with epoxy groups so that this flame retardant is incorporated into the epoxy network and reduces the glass transition temperature the least. Moisture uptake was determined by storing samples in water at 70 °C for 14 days. The increase in mass compared to the initial mass is 2% for the pure RTM6 and all other samples. According to this, the flame retardants have no influence on the moisture uptake. Glass transition temperatures of wetted samples ($T_{g,wet}$) are similar to the temperatures of the original samples, because drying occurs before the glass temperature is reached.

### 3.2. Thermal properties

The thermal properties of the flame retardants and RTM6 formulations thereof were investigated by TGA under nitrogen atmosphere and in air. Fig. 2 shows one step decomposition processes for RTM6 and flame retarded formulations in $N_2$-atmosphere on the left hand side and two step decomposition processes in air on the right hand side. The temperature at maximum mass loss rate ($T_{max}$), the initial degradation temperatures ($T_{1\%}$, $T_{5\%}$) at which 1% or 5% mass loss is reached and the residue at 800 °C are summarized in Table 3.

Under $N_2$-atmosphere the initial degradation temperatures $T_{1\%}$ and $T_{5\%}$ are lowered for every flame retardant which indicates a flame retarding action before the decomposition of the overall matrix. The residues are higher for flame retarded samples indicating the formation of char. As expected, it is highest for RDP with 23% which is more than the residue of RTM6 (9%) added to the amount of flame retardant incorporated into the matrix (10%). The high residue shows a strong charring effect of RDP in RTM6 resulting from the formation of polyphosphoric acid and the catalysis of the carbonization of the resin [37,38]. This charring layer is efficient to form a heat-barrier during combustion. RTM6 samples with added HFC-X and SPB100 show higher residues than neat RTM6 as well.

The simplified decomposition model by Rose and co-workers [39,40] assumes three steps for the decomposition of epoxy resins in air. An undistinctive first step is caused by dehydration leading to the formation of a moisture-free resin system. This step is not present in the measurements carried out. As shown above, moisture uptake is low for RTM6. In a temperature range of 300 °C to 450 °C the decomposition into stable char and different volatile species takes place. The third reaction taking place at temperatures above 450 °C is responsible for further degradation of the stable char. For RTM6 and RTM6 + 10% SPB100, more volatiles are set

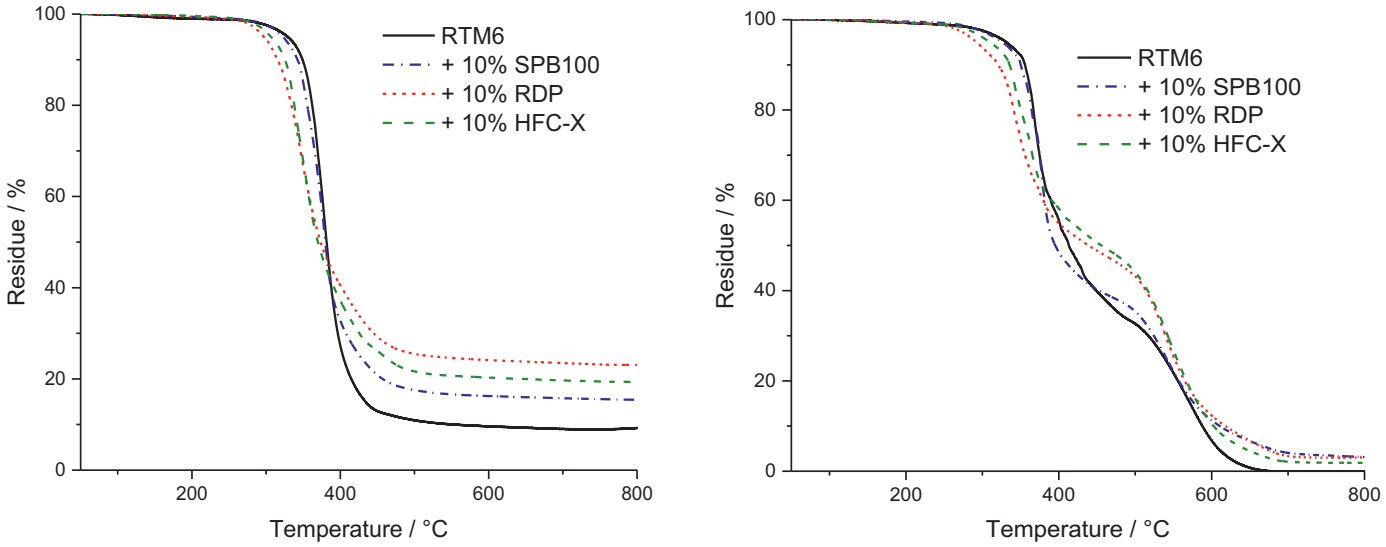


**Fig. 2.** TG-curves of RTM6 and flame retarded samples measured in $N_2$-atmosphere (left) and air (right). (For interpretation of the references to colour in this figure legend, the reader is referred to the web version of this article.)

**Table 4**
Rheological data of selected resin formulations (dynamic measurements, 1 K·min$^{-1}$, 1 s$^{-1}$).

| Formulation | *T(\|η*\| = 100 mPa·s)* / °C | *T(gel point, dynamic)* / °C |
|---|---|---|
| **RTM6** | 90 | 180 |
| + 10% RDP | 101 | 187 |
| + 10% HFC-X | 112 | 179 |
| + 10% SPB100 | 103 | 190 |

**Table 5**
ILSS of selected CFRP samples additionally normalized to RTM6 + CF.

| Sample | *ILSS* / N·mm$^{-2}$ | *Relative ILSS* / % |
|---|---|---|
| **RTM6 + CF** | 67.8 ± 3.2 | 100 ± 5 |
| + 5% RDP \| + 10% RDP | 69.2 ± 1.7 \| 68.8 ± 1.6 | 102 ± 3 \| 101 ± 2 |
| + 10% HFC-X | 62.9 ± 1.4 | 93 ± 2 |
| + 10% SPB100 | 66.0 ± 1.3 | 97 ± 2 |

free in the first distinctive step, leading to fewer residues before the second step occurs suggesting gas-phase activity for SPB100 (see Table 3).

### 3.3. Rheological and mechanical properties

For high-performance applications of RTM6 composite materials, it is important that the processibility by resin transfer moulding as well as mechanical properties are not affected by flame retardants incorporated to the matrix. Table 4 shows rheological data of dynamic measurements (heating rate 1 K·min$^{-1}$). In general, the injection temperature is 90 °C for RTM6 using processes. At this temperature, RTM6 reaches a viscosity of 100 mPa·s. For flame retardant formulations, it is important, that this viscosity can be reached by heating, while the possible potting time remains over 1 h. The values for the required temperatures *T(|η*| x003D; 100 mPa·s))* are given in Table 4 as well as the temperature at the dynamic gel point *T(gel point, dynamic)* determined at the intersection of storage modulus (*G'*) and loss modulus (*G''*) of the same dynamic measurements. Flame retardant formulations require higher temperatures to reach a viscosity of 100 mPa·s. Especially HFC-X with the highest molar mass increases the temperature by 22 °C. An additional isothermal measurement of RTM6 at 120 °C shows, that it is still processible for an adequate amount of time (> 1 h), so that the examined formulations are still suitable for resin transfer moulding. The gel point is only increased by a maximum of 10 °C, which does not affect the hardening process.

Table 5 presents interlaminar shear strength (*ILSS*) of the investigated CFRP samples. Values are additionally normalized to the CFRP without flame retardants. There is no influence of RDP on the *ILSS* observed up to a content of 10%. CFRP with 10% HFC-X or 10% SPB100 exhibit a slight reduction of *ILSS*, which is however not significant within the measurement tolerance of the testing method (± 10%). Therefore the application of the investigated flame retardants in epoxy based composites is possible with respect to mechanical performance.

### 3.4. Flame-retardant performance

Fire tests of the neat resin (4 mm samples) under forced conditions were done at a heat flux of 35 kW·m$^{-2}$ in a cone calorimeter. This heat flux is suitable for the investigation of the burning behavior. Composite materials (2 mm samples and 4 mm samples) were investigated at a heat flux of 60 kW·m$^{-2}$ respectively to quantifiably observe the fiber degradation within 20 min. The *HRR* (heat release rate) curves vs. time of neat resins are presented in Fig. 3 on the left hand side and the curves of the composites (2 mm) on the right hand side. Values of important parameters including time to ignition (*tti*), peak of heat release rate (*pHRR*), total heat release (*THR*), maximum average rate of heat emission (*MARHE*) and the total smoke release (*TSR*) values are summarized in Table 6. *MARHE* is an established parameter in cone calorimetry analysis that describes the velocity of the burning. For the 2 mm reinforced samples the sum parameters were determined after 300 s of testing and for the 4 mm neat resin samples after 500 s. Hand lay-up leads to different fiber volume ratios, so the combustible material amount differs for the different reinforced samples, which is considered by the value *X* as the ratio of the combustible material mass (equal to the mass of the matrix) to the whole sample mass. In addition UL94-test classifications of 4 mm thick samples are specified in Table 6.

The burning behavior of neat RTM6 is characterized by a sharp peak in *HRR*, which is characteristic for a rapid and continous combustion. For flame retarded samples the development of the *HRR* during the measurement shows a lower heat release shortly af-

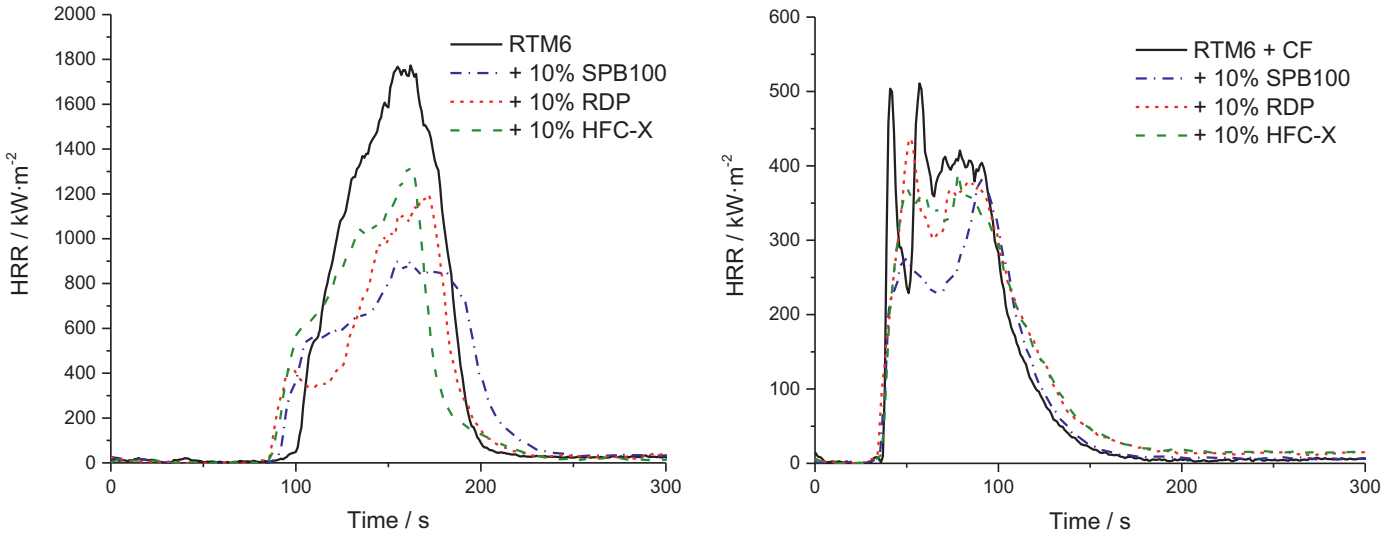


**Fig. 3.** *HRR* of non-reinforced samples at 35 kW·m$^{-2}$ (left) and of reinforced samples at 60 kW·m$^{-2}$ (right).

**Table 6**
Results of cone calorimetry (neat resin: sample thickness 4 mm, composites: sample thickness 2 mm) and classifications according to UL94-vertical tests (sample thickness 4 mm).

| Sample | *tti* / s | R / kW·m$^{-2}$ / kW·m$^{-2}$ | *THR·X$^{-1}$* / MJ·m$^{-2}$ | MARHE / kW·m$^{-2}$ / kW·m$^{-2}$ | *TSR·X$^{-1}$* / m$^2$·m$^{-2}$ | *THR·ML* m$^{-2}$·g / kW·m$^{-2}$·g$^{-1}$ / kW·m$^{-2}$·g$^{-1}$ | *Residue* / % | *X* | UL94-V |
|---|---|---|---|---|---|---|---|---|---|
| **RTM6** | 94 ± 1 | 1715 ± 58 | 104 ± 1 | 550 ± 6 | 5601 ± 31 | 2.25 | 4 ± 2 | 1 | NR* |
| + 10% RDP | 82 ± 3 | 1479 ± 284 | 77 ± 5 | 373 ± 11 | 2704 ± 148 | 2.22 | 37 ± 1 | 1 | V0 |
| + 10% SPB100 | 85 ± 1 | 882 ± 35 | 76 ± 1 | 362 ± 5 | 6441 ± 198 | 1.71 | 12 ± 1 | 1 | V0 |
| + 10% HFC-X | 79 ± 1 | 1331 ± 8 | 82 ± 1 | 430 ± 8 | 5563 ± 236 | 1.88 | 14 ± 1 | 1 | V0 |
| **RTM6 + CF** | 31 ± 2 | 492 ± 19 | 72 ± 1 | 242 ± 5 | 3763 ± 165 | 2.51 | 59 ± 1 | 0.43 | V0 |
| + 10% RDP | 30 ± 1 | 452 ± 26 | 67 ± 3 | 230 ± 15 | 4465 ± 443 | 2.40 | 60 ± 1 | 0.46 | V0 |
| + 10% SPB100 | 30 ± 0 | 413 ± 28 | 59 ± 2 | 194 ± 18 | 4978 ± 309 | 2.18 | 61 ± 3 | 0.45 | V0 |
| **+ 10% HFC-X** | 30 ± 1 | 428 ± 45 | 65 ± 4 | 229 ± 20 | 5193 ± 411 | 2.01 | 54 ± 2 | 0.53 | V0 |

*NR: not rated || Concentrations refer to the matrix material.
X: ratio of the combustible material mass (resin + flame retardant) to the whole sample mass.

ter burning, resulting in a peak maximum at a comparable time to the non-flame retarded sample. The addition of flame retardants to RTM6 leads to decreasing *tti*-values, but most importantly also decreasing *pHRR*-, *THR*- and *MARHE*-values. The reduction of *pHRR* is the highest for the sample flame retarded with SPB100 by 49%. In particular the addition of RDP leads to a decrease of the *HRR* just after ignition which is essential for the further burning process as the decrease of *HRR* indicates the formation of char [34].

UL94 measurements show that an addition of 10 wt% of flame retardants results in V0 classifications for all samples. The fiber reinforcement acts as inert filler. Therefore, the RTM6-composite reaches V0 classification even without an additional flame retardant. Literature [2] showed that 3 mm thick composites of RTM6 reach no rating.

The fiber-reinforcement leads to significant differences in the *HRR*-curves in comparison to non-reinforced material. Delamination processes are represented in the curves by sharp peaks shortly after ignition. Single plies are detached from others and they burn fierce and fast due to gas between the fiber plies acting as a heat barrier. This process is suppressed by the incorporation of flame retardants resulting in less sharp peaks of the *HRR*-curves. The reinforcement significantly reduces *pHRR, THR, MARHE* and *TSR*. The relative changes caused by the incorporation of flame retardants are comparable to the non-reinforced samples, however less pronounced due to lower base values and higher heat flow.

The *THR/ML* (*ML* = mass loss) value gives reliable information on the flame retardant mechanism [34] as it stands for the total heat evolved per mass that is released in form of volatiles. The smaller this value is in comparison to the non-flame retarded sample, the more gas phase activity occurs during combustion. According to the value of *THR/ML*, RDP acts mainly in the condensed phase (flame retarded neat resin sample: 2.22 kW·m$^{-2}$·g$^{-1}$ / non flame retarded RTM6 sample: 2.25 kW·m$^{-2}$·g$^{-1}$) which is also shown by a high residue of the non-reinforced sample (37%) and the low *TSR·X$^{-1}$* (2704 m$^2$·m$^{-2}$) as well as the TGA results. SPB100 and HFC-X show a distinctive gas phase activity with values of 1.71 kW·m$^{-2}$·g$^{-1}$ and 1.88 kW·m$^{-2}$·g$^{-1}$, respectively. The values of carbon fiber reinforced samples show a similar tendency, that RDP acts mainly in the condensed phase (flame retarded reinforced sample: 2.40 kW·m$^{-2}$·g$^{-1}$ / non flame retarded RTM6 sample: 2.51 kW·m$^{-2}$·g$^{-1}$) and SPB100 and HFC-X act mainly in the gas phase (2.18 kW·m$^{-2}$·g$^{-1}$ and 2.01 kW·m$^{-2}$·g$^{-1}$). It is remarkable, that HFC-X shows more gas phase activity than SPB100 in the reinforced samples, whereas it is the other way around in non-reinforced RTM6 samples. This shows, that the flame retarding mechanism is slightly changed by the incorporation of fibers.

The overall amount of formed smoke (*TSR·X$^{-1}$*) is higher for flame retarded composite samples than for the non-flame retarded samples. The best flame retardancy regarding *THR* and *pHRR* is generated by the intumescent SPB100. The intumescence is suppressed in the composite material, but the resulting residue and the gas-phase active volatile products are sufficient for an efficient flame retardancy. Especially the results for the DOPO-containing flame retardant HFC-X is remarkable as DOPO itself is said to be a very good flame retardant for carbon fiber reinforced epoxy resins. To estimate a flame retardant efficiency, plenty of parameters have

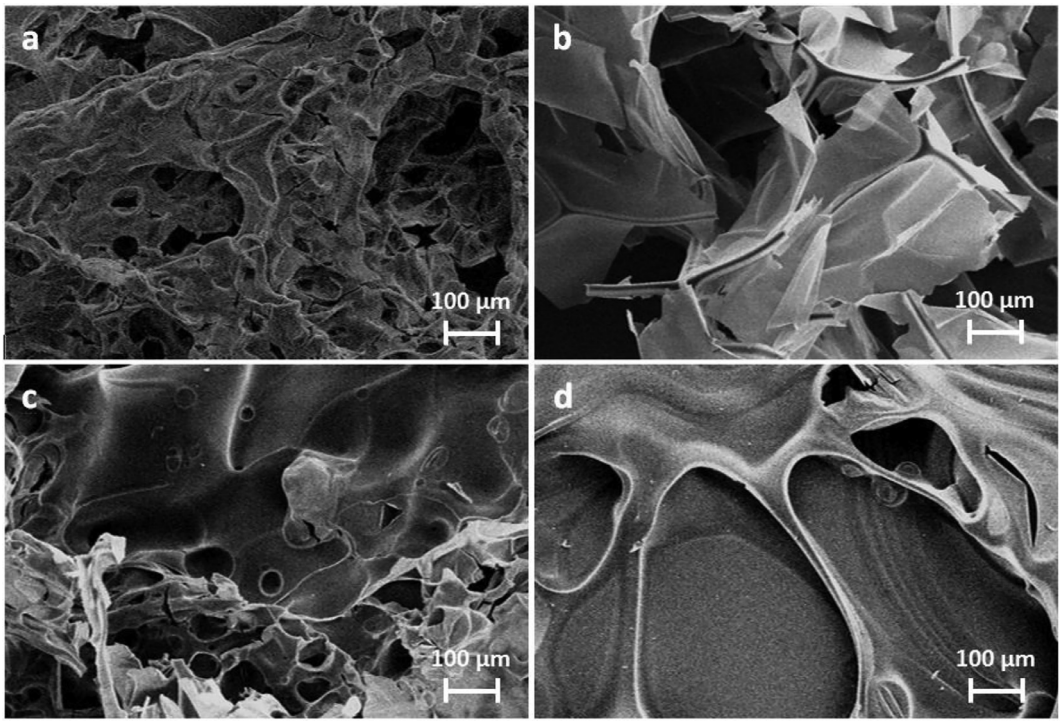


**Fig. 4.** SEM images of the residues obtained after cone calorimetry at 35 kW·m$^{-2}$ for 10 min: a: RTM6, b: RTM6 + 10% RDP, c: RTM6 + 10% SPB100, d: RTM6 + 10% HFC-X.

**Table 7**
Mean diameter, standard deviation and smallest measured diameter of at least 30 carbon fibers in composite materials with partially flame retarded RTM6 after irradiation at 60 kW·m$^{-2}$ for 20 min determined by SEM.

| Sample | *Thickness* / mm | *Mean Diameter* / µm | *Smallest Diameter* / µm |
|---|---|---|---|
| **RTM6 + CF** | 2 | 3.3 ± 0.7 | 2.1 |
| + 5% RDP | 2 | 5.8 ± 0.3 | 5.3 |
| + 10% RDP | 2 \| 4 | 6.2 ± 0.2 \| 6.2 ± 0.4 | 5.7 \| 5.4 |
| + 5% HFC-X | 2 | 5.5 ± 0.2 | 5.0 |
| + 10% HFC-X | 2 \| 4 | 5.6 ± 0.3 \| 5.6 ± 0.3 | 4.9 \| 5.2 |
| + 4% SPB100 | 2 | 5.4 ± 0.5 | 4.0 |
| + 10% SPB100 | 2 \| 4 | 5.9 ± 0.4 \| 5.9 ± 0.4 | 5.4 \| 4.9 |
| + 15% SPB100 | 2 | 5.9 ± 0.4 | 4.9 |

to be taken into account. In HFC-X, DOPO is incorporated to a polymer chain. This has a positive influence on migration or thermal properties but may have an influence on flame retardant properties in comparison to molecular DOPO as well, as can be seen in these studies.

Fig. 4 shows SEM images of the residues obtained after cone calorimetry at 35 kW·m$^{-2}$ for 10 min (non-reinforced samples). While RTM6 itself forms a highly instable residue that contains small holes (diameter about 50 – 100 µm), the addition of phosphorus containing flame retardants leads to residues that are more stable and contain less holes. This confirms the observations from cone calorimetry tests and UL94 measurements.

### 3.5. Fiber protection

The mean diameters and the smallest fiber diameters of carbon fibers on the irradiated sample surface shown in Table 7 were determined by SEM. The determined initial diameter of the G0939 fiber is (7.3 ± 0.3) µm. For composites not containing any flame retardant a mean fiber diameter of (3.3 ± 0.7) µm and a mentionable amount of respirable fiber fragments are observed after irradiation (20 min at 60 kW·m$^{-2}$). The incorporation of any investigated flame retardant causes larger mean fiber diameters. The values show no influence of the sample thickness on the fiber degradation. For example, if 10% SPB100 in RTM6 is used as matrix, fiber diameters of (5.9 ± 0.4) µm are obtained for 2 mm and 4 mm samples. An increase of the amount of incorporated flame retardant shows typically no significant increase of the mean fiber diameter. For example the incorporation of 4% SPB100 in the RTM6 matrix generates fibers with a mean diameter of (5.4 ± 0.5) µm whereas 10% SPB100 cause a mean diameter of (5.9 ± 0.4) µm. A further increase to 15% SPB100 shows no additional effect. In comparison to SPB100, RDP shows slightly higher mean fiber diameters after irradiation whereas HFC-X shows lower mean fiber diameters. The sample with 5% RDP shows a mean fiber diameter of (5.8 ± 0.3) µm and 5% HFC-X (5.5 ± 0.2) µm. The best result is obtained by the addition of 10% RDP to the matrix with a mean fiber diameter of (6.2 ± 0.4) µm. The comparable sample with 10% HFC-X generates fibers with a mean diameter of (5.6 ± 0.3) µm. An amount of 5% flame retardant in the RTM6 matrix is sufficient for every sample to avoid formation of respirable fiber fragments according to the WHO whereas the non-flame retarded sample show fibers with diameters below 3 µm.

Fig. 5 shows the mean fiber diameter in dependence on irradiation time at 60 kW·m$^{-2}$ for different resin formulations. The samples without flame retardants show a steady decrease of the mean fiber diameter. After 5 min a mean diameter of (6.6 ± 0.4) µm is reached, after 20 min (3.3 ± 0.7) µm. By adding flame retardants,

**Table 8**
Concentrations of elements at the fiber surface after irradiation.

| Sample | C on surface / % | N on surface / % | O on surface / % | P on surface / % |
|---|---|---|---|---|
| **RTM 6 + CF: 1200 s at 60 kW·m$^{-2}$** | 94.3 | 4.2 | 1.4 | not detected |
| + 10% RDP: 300 s at 60 kW·m$^{-2}$ | 82.5 | 3.7 | 6.6 | 5.3 |
| + 10% RDP: 600 s at 60 kW·m$^{-2}$ | 86.4 | 5.3 | 6.5 | 1.8 |
| + 10% RDP: 1200 s at 60 kW·m$^{-2}$ | 86.4 | 4.2 | 7.1 | 1.3 |
| + 10% RDP: 1500 s at 60 kW·m$^{-2}$ | 89.1 | 5.2 | 4.4 | 0.9 |
| + 10% SPB100*: 1200 s at 60 kW·m$^{-2}$ | 90.5 | 6.5 | 2.6 | 0.4 |
| + 10% HFC-X: 1200 s at 60 kW·m$^{-2}$ | 90.2 | 5.1 | 3.7 | 0.8 |

*For this sample a residue of spherical particles (C: 3.2%, $N < 0.1$%, O: 50.4%, P: 19.3%) were observed on the fiber surface.

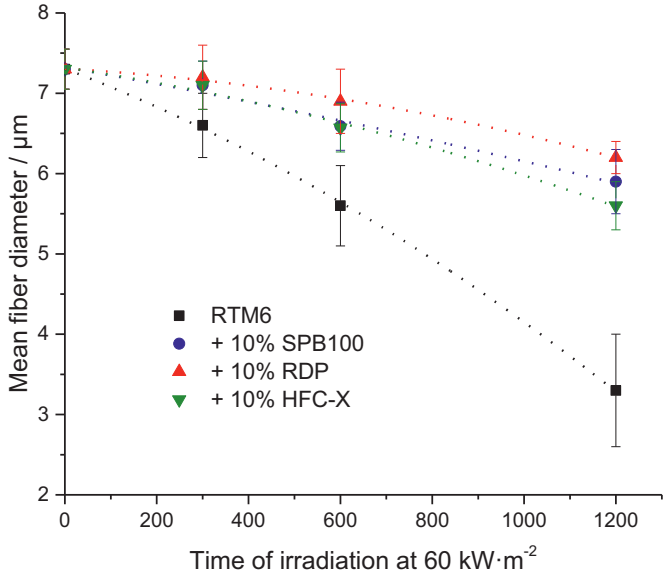


**Fig. 5.** Mean fiber diameter in dependence on irradiation time at 60 kW·m$^{-2}$ and flame retarded matrix composition.

the degradation is retarded sufficiently within the observed irradiation time of 1200 s. Especially up to 300 s there is no significant degradation of the fiber diameter. The progression of the curves is similar for all flame retardants used. An additional composite containing 10% RDP that was irradiated for 1500 s exhibits still a mean diameter of (5.3 ± 0.3) µm (not depicted in Fig. 5). Fig. 6 shows SEM images of carbon fibers after irradiation at 60 kW·m$^{-2}$. While the composite which does not contain any flame retardants (Fig. 6; a) tends to form holes at the fiber surface within 1200 s, the sample with 10% RDP shows no defects after 1500 s (b).

In order to determine the mechanism of fiber protection, the temperature on the irradiated surface during combustion was measured by a thermocouple attached to the sample. The results are shown in Fig. 7. Temperatures above 600 °C necessary for fiber degradation (12) are reached during the combustion of the matrix resin. There are no distinct differences in the shape of these curves suggesting that there is no influence of the surface temperature on the resulting mean fiber diameter, but the added flame retardants are responsible for fiber protection. The temperature measurement is not exact but sufficient for a comparison and the temperature differences that have to be reached for the observed increase in fiber diameter would be observable. No tape is stable enough to stick to the sample surface throughout the whole measurement, but the thermocouple placement via tape beforehand leads to it steadily laying on top of the sample surface for at least 300 s. This has been observed for every measurement used in this report.

The results of EDX measurements are summarized in Table 8. After 1200 s at 60 kW·m$^{-2}$ the surface of carbon fibers in the non flame retarded composite sample consists of 94.3% carbon, 4.2% nitrogen and 1.4% oxygen. The incorporation of 10% RDP to RTM6 changes the composition to 86.4% carbon, 4.2% nitrogen, 7.1% oxygen and 1.3% phosphorus. For this sample, different irradiation times were investigated and it is shown that the phosphorus content is decreasing from 5.3% after 300 s to 0.9% after 1500 s. For RDP the primary fire retardant action is likely to occur in the condensed phase by the formation of polyphosphoric acid [17,18]. However, with prolonged irradiation polyphosphoric acid is degraded and fiber protection decreases. HFC-X and SPB100 also lead to phosphorus containing residues directly on the carbon fibers. Fig. 8a shows a SEM-EDX image of a carbon fiber of the sample containing 10% SPB100 after irradiation for 20 min. Wider blue phosphorus-rich areas (for example spherical particles consisting of 3.2% carbon, 50.4% oxygen, 19.3% phosphorus) and light blue areas evenly spread inside the red carbon-rich area on the carbon fibers. This means, that phosphorus containing compounds are found all over the fiber but in very small dimensions and amounts. This is consistent to observations described in literature. A study [41] showed, that graphite can be protected from oxidation by impregnation with organic phosphate and phosphite esters. The thermal decomposition of phosphorus compounds leaves a hydrophilic residue strongly adsorbed on the graphite surface. The authors assume a covalent bonding to the graphite surface in form of C–$OPO_3$ groups leading to a hydrophilic surface. Additionally, during the irradiation under the cone heater a loose matrix residue is obtained on top of the sample and between the laminate plies that is decreased constantly during the run. The carbon fiber fabric additionally contains few colored glass fibers for orientation while processing. A glass fiber of the fiber ply shows a continuous phosphorus containing layer on its surface (Fig. 8b). Therefore the residue is hydrophilic as expected due to the formation of pyrophosphates from the phosphorus containing flame retardants. The image of the carbon fiber mentioned above does not present a continuous, thick protection layer due to its unpolar character (Fig. 8a).

### *3.6. Silicon dioxide: Influence on flame retardancy and fiber protection*

Nanopox F400 (NPF400) was used to investigate if silicon dioxide may protect the fibers from thermal degradation as well. It consists of silicon dioxide particles with a diameter of 20 nm

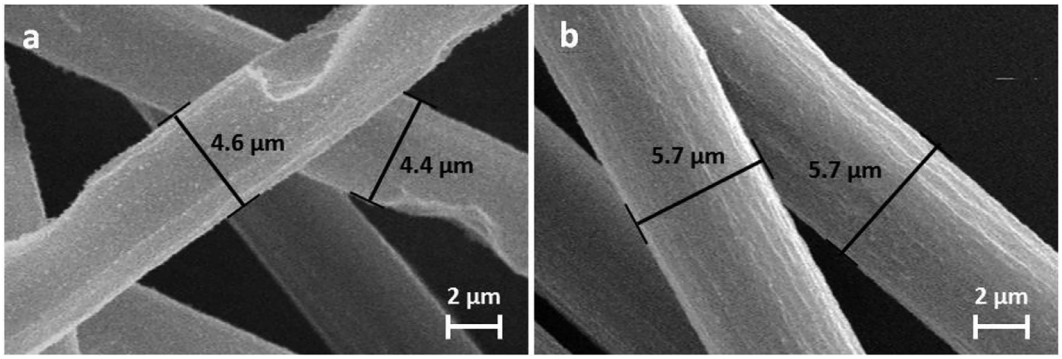


**Fig. 6.** SEM images of carbon fibers after irradiation at 60 kW·m$^{-2}$: a: RTM6 + CF, 1200 s; b: RTM6 + 10% RDP, 1500 s.

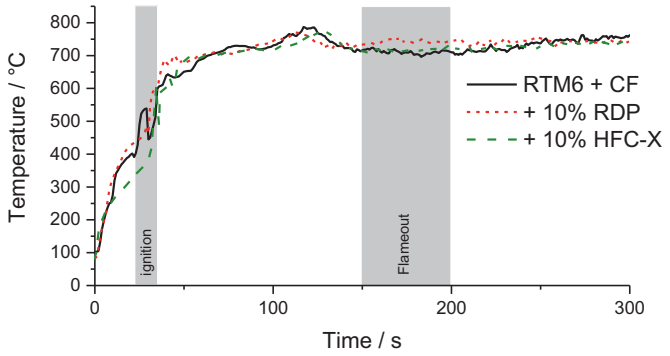


**Fig. 7.** Temperature at the sample surface during irradiation (60 kW·m$^{-2}$) measured by a thermocouple attached to the surface. (For interpretation of the references to colour in this figure legend, the reader is referred to the web version of this article.)

evenly dispersed in a stable mixture with bisphenol a diglycidyl ether, so it is miscible with RTM6 and suitable for resin transfer moulding processes. Silicon dioxide is a filler that can act in the condensed phase by creating a barrier for heat and oxygen. As literature (see above) describes a synergism of silicon and phosphorus in regard to flame retardancy, SPB100 was chosen for combinations thereof.

Fire tests of the composite materials (thickness 2 mm) under forced conditions were done at a heat flux of 60 kW·m$^{-2}$ in a cone calorimeter to observe fiber degradation and burning behavior. The *HRR* (heat release rate) curves are presented in Fig. 9. Values of important parameters including time to ignition (*tti*), peak of heat release rate (*pHRR*), total heat release (*THR*), maximum average rate of heat emission (*MARHE*) and the total smoke release (*TSR*) values are summarized in Table 9. For these samples, the sum parameters were determined after 300 s of testing and concentrations refer to the matrix material. Hand lay-up leads to different fiber volume ratios, so the combustible material amount differs for the different reinforced samples, which is considered by the value *X* as the ratio of the combustible material mass (equal to the mass of the matrix) to the whole sample mass.

The addition of 10% NPF400 to the epoxy matrix leads to higher *pHRR, THR* and *MARHE.* So it shows no flame retarding properties. The *pHRR* is 492 kW·m$^{-2}$ for RTM6 and 566 kW·m$^{-2}$ for 10% NPF400 in RTM6. *THR* (normalized by *X*) increases from 72 MJ·m$^{-2}$ to 79 MJ·m$^{-2}$ and *MARHE* from 242 kW·m$^{-2}$ to 267 kW·m$^{-2}$. Formulations containing both, NPF400 and SPB100, show similar *HRR* curves to formulations with 10% SPB100. Delamina-

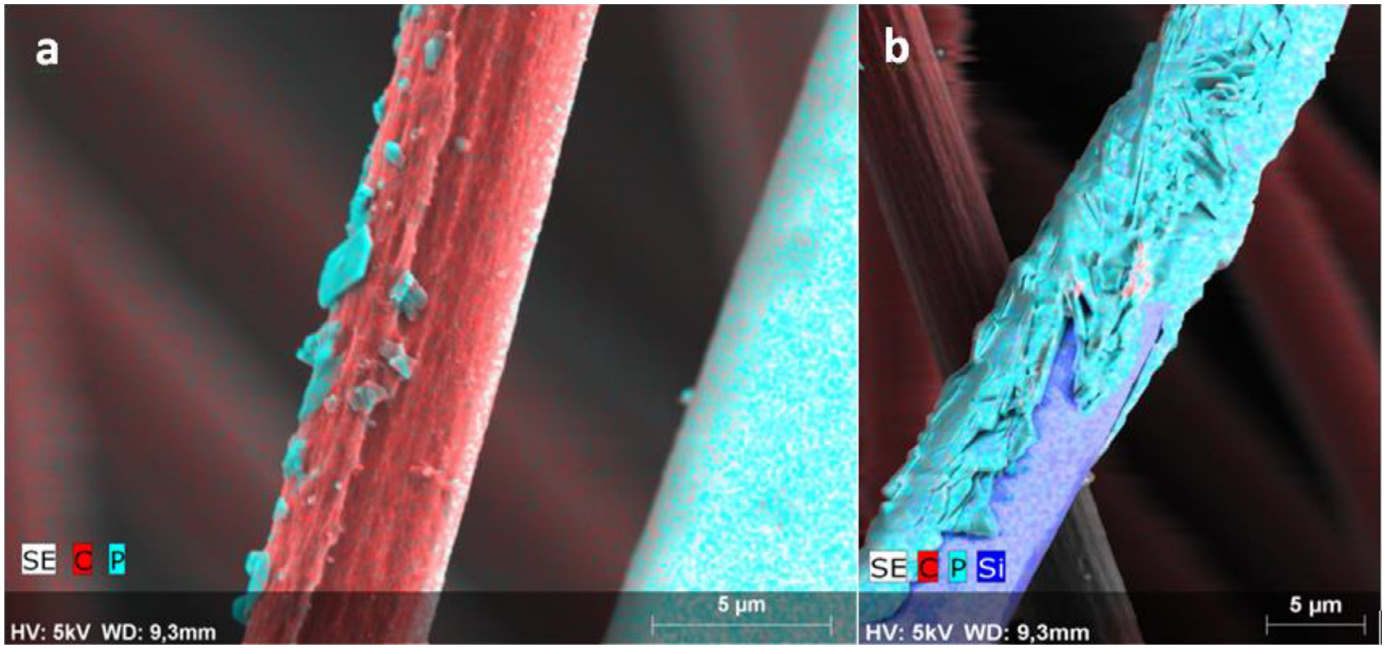


**Fig. 8.** SEM-EDX images of a: carbon fiber and b: glass fiber (RTM6 + 10% SPB100 + CF) after irradiation at 60 kW·m$^{-2}$ for 20 min.

**Table 9**
Results of cone calorimetry (sample thickness 2 mm) and classifications according to UL94-vertical tests (sample thickness 4 mm) for investigated samples.

| Sample | *tti* / s | R / kW·m$^{-2}$ / kW·m$^{-2}$ | *THR·X$^{-1}$* / MJ·m$^{-2}$ | RHE / kW·m$^{-2}$ / kW·m$^{-2}$ | *TSR·X$^{-1}$* m$^2$·m$^{-2}$ | *THR·ML$^{-1}$W·m$^{-2}$·g$^{-1}$* / kW·m$^{-2}$·g$^{-1}$ | *Residue* / % | *X* | UL94-V |
|---|---|---|---|---|---|---|---|---|---|
| **RTM6 + CF** | 31 ± 2 | 492 ± 19 | 72 ± 1 | 242 ± 5 | 3763 ± 165 | 2.51 | 59 ± 1 | 0.43 | V0 |
| + 10% SPB100 | 30 ± 0 | 413 ± 28 | 59 ± 2 | 194 ± 18 | 4978 ± 309 | 2.18 | 61 ± 3 | 0.45 | V0 |
| + 10% NPF400 | 28 ± 2 | 566 ± 21 | 79 ± 1 | 267 ± 5 | 4319 ± 105 | 2.78 | 59 ± 1 | 0.46 | V0 |
| + 5% SPB100 + 5% NPF400 | 30 ± 2 | 368 ± 45 | 58 ± 4 | 193 ± 18 | 4828 ± 249 | 2.37 | 66 ± 3 | 0.44 | V0 |
| + 7% SPB100 + 3% NPF400 | 28 ± 2 | 437 ± 32 | 60 ± 2 | 203 ± 4 | 4308 ± 162 | 2.21 | 62 ± 1 | 0.42 | V0 |

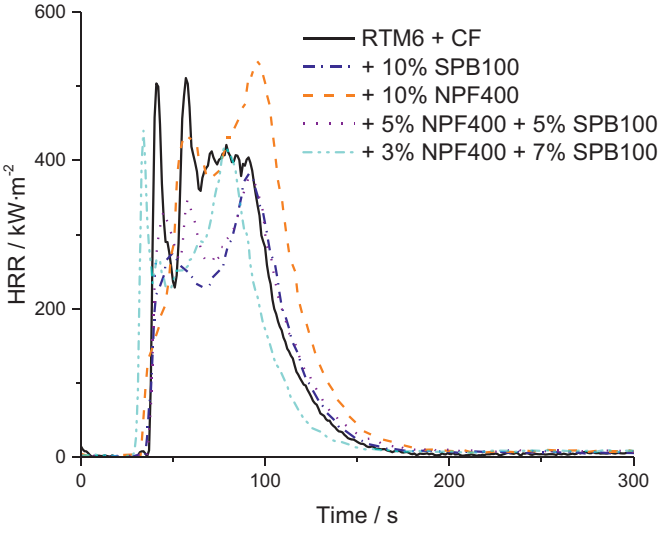


**Fig. 9.** *HRR* of reinforced samples at 60 kW·m$^{-2}$ including silicon compounds.

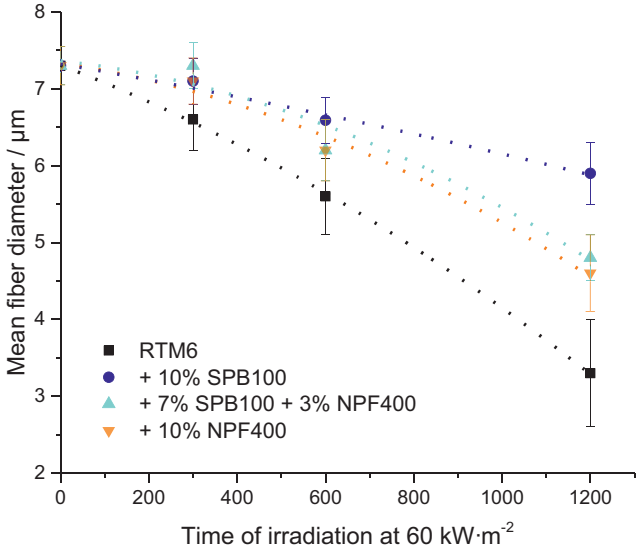


**Fig. 10.** Mean fiber diameter in dependence on irradiation time at 60 kW·m$^{-2}$ and flame retarded matrix composition including silicon compounds.

**Table 10**
Mean diameter, standard deviation and smallest measured diameter of at least 30 carbon fibers in composite materials (thickness 2 mm) with silicone compounds after irradiation at 60 kW·m$^{-2}$ for 20 min determined by SEM.

| Sample | *Mean Diameter* / µm | *Smallest Diameter*/ µm |
|---|---|---|
| **RTM6 + CF** | 3.3 ± 0.7 | 2.1 |
| + 4% SPB100 | 5.4 ± 0.5 | 4.0 |
| + 10% SPB100 | 5.9 ± 0.4 | 5.4 |
| + 10% NPF400 | 4.6 ± 0.5 | 3.9 |
| + 3% NPF400 + 7% SPB100 | 4.8 ± 0.3 | 4.2 |

tions are mainly observed for samples containing NPF400 as flame retardant component, showing unsteady combustion. The value of *THR·ML$^{-1}$* decreases with increasing amount of SPB100 from 2.51 MJ·m$^{-2}$·g$^{-1}$ without flame retardant to 2.37 MJ·m$^{-2}$·g$^{-1}$ with 5% SPB100 and 5% NPF400 and 2.21 MJ·m$^{-2}$·g$^{-1}$ for the formulation with 7% SPB100 and 3% NPF400 in the RTM6 matrix. This means, that gas phase activity increases with increasing amount of SPB100, what was expected. The flame retarding effect is mainly caused by SPB100 and no synergism of SPB100 and NPF400 can be observed in RTM6 and carbon fiber reinforced RTM6. The effects are similar in neat resin samples not shown in this study.

Table 10 summarizes mean diameters of carbon fibers for different samples after 20 min of irradiation at 60 kW·m$^{-2}$. NPF400 shows a fiber protecting effect, since the resulting mean fiber diameter is 4.6 µm (10% NPF400 in RTM6 matrix) and therefore higher than for the RTM6 sample (3.3 µm). No fragments with respirable dimensions were found. But NPF400 is less effective than SPB100 (5.9 µm, 10%). A mixture of 3% NPF400 and 7% SPB100 in the RTM6 matrix shows a lower mean fiber diameter (4.8 µm) than a formulation with only 4% SPB100. This shows, that there is an antagonism in regard to fiber protection. Fig. 10 shows the mean fiber diameter in dependence on irradiation time. Both silicon containing formulations show a similar curve. These curves show a faster carbon fiber degradation than samples containing only SPB100 as flame retardant, again supporting the antagonistic effect of the silicon incorporation.

SEM-EDX images of fibers after irradiation at 60 kW·m$^{-2}$ for 20 min are shown in Fig. 11. The sample containing 10% NPF400 in the matrix formulation (Fig. 11, left) shows only loose, silicon containing thin layer-like residues on the fibers. Similar residues are formed on the sample containing 5% SPB100 and 5% NPF400 in the matrix (Fig. 11, right). These residues do not offer a sufficient protection from heat and oxygen and therefore from the thermo-oxidative degradation. The 10% NPF400 sample shows element concentrations determined by SEM-EDX of 97.5% carbon, 2.5% oxygen and less than 0.1% silicon on the exposed fiber surface after irradiation. The corresponding loose residue on top consists of 35.1% carbon, 37.8% oxygen and 27.1% silicon. The values for the sample with 5% SPB100 and 5% NPF400 are 96.1% carbon, 3.9% oxygen, less than 0.1% silicon and less than 0.1% phosphorus on the exposed fibers and for the corresponding loose silicon containing residue 11.2% carbon, 49.9% oxygen, 38.4% silicon and 0.5% phosphorus. This shows, that the silicon compound binds phosphorus compounds formed during combustion. In other words, the formed hydrophilic phosphorus compounds show a higher affinity to the hydrophilic silicon compounds deriving from NPF400 or glass fibers than to carbon fibers. This high affinity is also shown by literature [42] describing the formation of –P(=O)–O–Si– structures as important mode of action for the flame retardant synergism of phosphorus and silicon, and is also consistent with the higher stability of organic phosphoric acid esters compared to silicic acid esters.

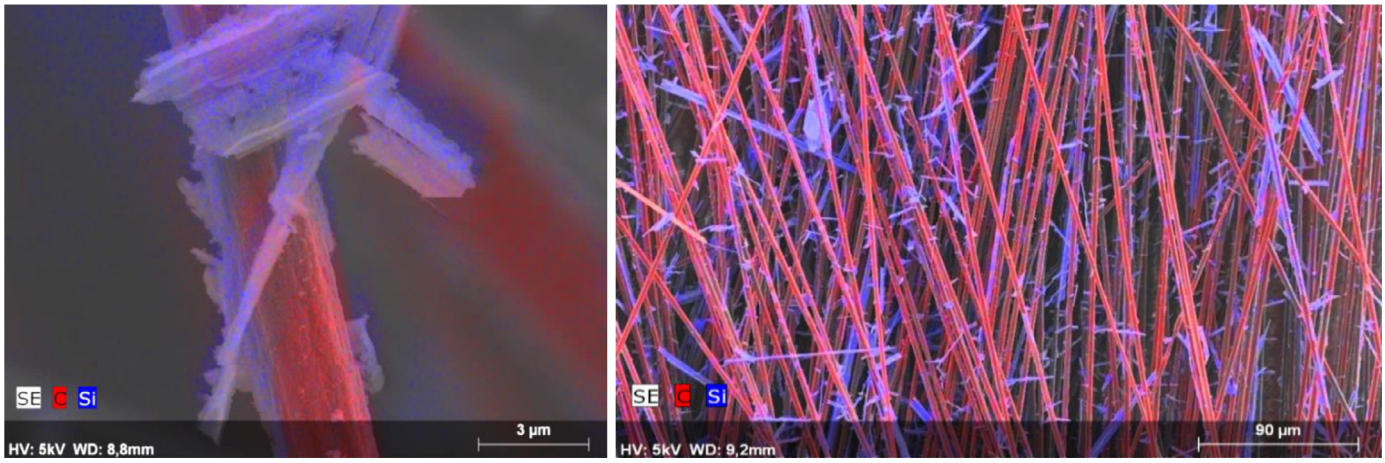


**Fig. 11.** SEM-EDX images of residual fibers after irradiation at 60 kW·m$^{-2}$ for 20 min in the cone calorimeter. Left: carbon fiber reinforced sample with 10% NPF400 incorporated to the matrix, right: carbon fiber reinforced sample with 5% SPB100 and 5% NPF400 incorporated to the matrix.

In presence of silicon containing compounds, there are no areas with high phosphorus content on the carbon fiber surface as could be found for the sole phosphorus containing flame retardants above. Therefore, the phosphorus compounds are not available for fiber protection anymore. This verifies that the high fiber protection efficiency of phosphorus containing flame retardants is not only due to a loose residue on top of the samples. It is caused by phosphorus compounds that are evenly and continuously spread on the fiber surface after combustion of the matrix and still exist after 1200 s of irradiation at 60 kW·m$^{-2}$ as already suggested above.

## 4. Conclusions

Different phosphorus containing flame retardants were investigated with regard to flame retardancy in the neat RTM6 resin and in carbon fiber reinforced composite materials. The main focus was on the retardation of the fiber degradation leading to respirable fiber fragments with diameter below 3 µm. Cone calorimetric measurements were carried out at 35 kW·m$^{-2}$ for neat resin samples and at 60 kW·m$^{-2}$ for composite materials. A heat flux of 60 kW·m$^{-2}$ and an irradiation time of 20 min were necessary to quantifiably determine the fiber degradation. The phosphazene (SPB100) showed the best flame retardant efficiency in the composite, particularly with regard to a reduction of the *pHRR* of 51% in the neat resin when 10% flame retardant were added. The oligomeric phosphate (RDP) containing composite samples showed the best fiber protection with a mean fiber diameter of 6.2 ± 0.4 µm (10% RDP) in comparison to the non-flame retarded sample with a mean fiber diameter of 3.3 ± 0.7 µm after an irradiation time of 20 min. In contrast to the non-flame-retarded sample, the flame retardant containing samples showed no formation of defects at the fiber surface. In conclusion by incorporation of any investigated phosphorus containing flame retardant in amounts of 5 – 10% by matrix weight the fiber degradation can be retarded sufficiently. After 20 min of irradiation at 60 kW·m$^{-2}$ fiber diameters exclusively above 5 µm were obtained. Temperature measurements on the sample surface during irradiation showed no differences and therefore no relation of temperature and fiber degradation in these boundaries. The effect of fiber protection is at first view a result of a loose residue on the fibers and between the laminates. At second view, the fiber protection is caused by phosphorus compounds evenly spread over the carbon fiber surface.

By studying the incorporation of silicon compounds as well, further statements can be made in terms of the fiber protection mechanism. Silicon dioxide particles themselves show no flame retardancy and no synergism to SPB100 as well as a less efficient fiber protection in carbon fiber reinforced RTM6 samples. For silicon and phosphorus containing samples, loose silicon dioxide based residues are formed binding present phosphorus compounds. In contrast, samples without silicon compounds show areas containing phosphorus evenly spread on the irradiated carbon fiber surface and even if it is no continuous layer this is at second view the reason for the particular efficiency in fiber protection of phosphorus containing flame retardants. The affinity of phosphorus compounds to carbon fibers is higher than that of silicon compounds, leading to these protected areas directly on the fiber surface. But if silicon compounds are additionally incorporated, they bind formed phosphorus compounds during combustion, so these are not available for a fiber protection directly on the fibers, resulting in an antagonistic effect on fiber protection.

The effect of the flame retardant on the reaction to fire does not correlate with the effect on the fiber degradation. Whereas RDP that acts mainly in the condensed phase guarantees the best fiber protection, SPB100, that acts mainly in the gas phase, shows the best flame-retardant efficiency in the neat resin as well as in the fiber reinforced composite. HFC-X is the least favorable compound for both, flame retardancy and fiber reaction. For future research addressing the protection of carbon fibers in composites, the different flame retarding and fiber protection mechanisms in flame retardants as well as synergistic or antagonistic effects have to be considered.

The interlaminar shear strength was not affected significantly by the incorporation of flame retardants and consequently the use of the flame-retarded RTM6 in composite materials is still possible. This is supported by the glass transition temperatures that are still high enough and the hot-wet properties showing no change in glass transition temperatures and no additional moisture uptake.

## Declaration of Competing Interest

None.

## CRediT authorship contribution statement

**Lara Greiner:** Conceptualization, Investigation, Writing - original draft, Visualization. **Manfred Döring:** Writing - review & editing, Supervision. **Sebastian Eibl:** Conceptualization, Writing - review & editing, Supervision.

## References


[1] L. Zang, S. Wagner, M. Ciesielski, P. Müller, M. Döring, Novel star-shaped and hyperbranched phosphorus-containing flame retardants in epoxy resins, Polym. Adv. Technol. 22 (7) (2011) 1182–1191.

[2] B. Perret, B. Schartel, K. Stöß, M. Ciesielski, J. Diederichs, M. Döring, J. Krämer, V. Altstädt, A New Halogen-Free Flame Retardant Based on 9,10-Dihydro-9-oxa-10-phosphaphenanthrene-10-oxide for Epoxy Resins and their Carbon Fiber Composites for the Automotive and Aviation Industries, Macromol. Mater. Eng. 296 (1) (2011) 14–30.

[3] M. Döring, M. Ciesielski, C. Heinzmann, in: Synergistic Flame Retardant Mixtures in Epoxy resins. *Fire and Polymers VI: New advances in Flame Retardant Chemistry and Science*, American Chemical Society, Washington DC, 2012, pp. 295–309.

[4] M. Ciesielski, J. Diederichs, M. Döring, A. Schäfer, Advanced flame-retardant epoxy resins for composite materials. *Fire and Polymers V*, ACS Symp. Ser. 1013 (2009) 174–190.

[5] S.V. Levchik, G. Camino, L. Costa, M.P. Luda, Mechanistic study of thermal behaviour and combustion performance of carbon fibre-epoxy resin composites fire retarded with a phosphorous-based curing system, Polym. Degrad. Stab. (54) (1996) 317–322.

[6] F.J. Martin, K.R. Price, Flammability of epoxy resins, J. Appl. Polym. Sci. (12) (1968) 143–158.

[7] A. Toldy, B. Szolnoki, G. Marosi, Flame retardancy of fibre-reinforced epoxy resin composites for aerospace applications, Polym. Degrad. Stab. 96 (3) (2011) 371–376.

[8] S. Eibl, D. Reiner, M. Lehnert, Gefährdung durch lungengängige Faserfragmente nach dem Abbrand Kohlenstofffaser verstärkter Kunststoffe (Health hazards by respirable fiber fragments after combustion of carbon fiber reinforced plastic material), Gefahrstoffe - Reinhaltung der Luft 74 (2014) 7/8.

[9] Eibl, S. and Scholz, N. Besondere Gefährdung beim Abbrand von Carbon-Kunststoffen (Particular hazards Related to Combustion of Carbon Fiber Reinforced Plastic Material). Brandschutz, Deutsche Feuerwehr-Zeitung, 423–427.

[10] P.F. Holt, M. Horne, Dust from Carbon Fibre, Environ. Res. 17 (1978) 276–283.

[11] T. Hertzberg, Dangers relating to fires in carbon-fibre based composite material, Fire Mater. 29 (4) (2005) 231–248.

[12] S. Eibl, Potential for the formation of respirable fibers in carbon fiber reinforced plastic materials after combustion, Fire Mater. 41 (7) (2017) 808–816.

[13] World Health Organization Hazard prevention and Control in the Work Environment: Airborne dust: WHO/SDE/OEH/99.14. http://www.who.int/occupational_health/publications/en/oehairbornedust3.pdf (18 December 2017).

[14] S. Eibl, Flammgeschützte Kohlenstofffaser (Flame retardant Carbon Fiber), 2017 DE102015010001 A1.

[15] U. Braun, A.I. Balabanovich, B. Schartel, U. Knoll, J. Artner, M. Ciesielski, M. Döring, R. Perez, J.K. Sandler, V. Altstädt, T. Hoffmann, D. Pospiech, Influence of the oxidation state of phosphorus on the decomposition and fire behaviour of flame-retarded epoxy resin composites, Polymer 47 (26) (2006) 8495–8508.

[16] K.H. Pawlowski, B. Schartel, Flame retardancy mechanisms of triphenyl phosphate, resorcinol bis(diphenyl phosphate) and bisphenol A bis(diphenyl phosphate) in polycarbonate/acrylonitrile–butadiene–styrene blends, Polym. Int. 56 (11) (2007) 1404–1414.

[17] S.V. Levchik, D.A. Bright, G.R. Alessio, S. Dashevsky, New halogen-free fire retardant for engineering plastic applications, J. Vinyl Add. Tech. (7) (2001) 98–103.

[18] S.V. Levchik, D.A. Bright, P. Moy, S. Dashevsky, New developments in fire retardant non-halogen aromatic phosphates, J. Vinyl Add. Tech. (6) (2000) 123–128.

[19] C.W. Allen, The Use of Phosphazenes as Fire Resistant Materials, J. Fire Sci. (11) (1993) 320–328.

[20] F. Laoutid, L. Bonnaud, M. Alexandre, J.-.M. Lopez-Cuesta, P. Dubois, New prospects in flame retardant polymer materials: from fundamentals to nanocomposites, Mater. Sci. Eng.: R: Reports 63 (2009) 100–125.

[21] G.M. Wu, B. Schartel, D. Yu, M. Kleemeier, Hartwig A. Synergistic fire retardancy in layered-silicate nanocomposite combined with low-melting phenysiloxane glass, J. Fire Sci. 30 (2012) 69–87.

[22] S. Agrawal, A.K. Narula, Synthesis and characterization of phosphorus- and silicon-containing flame-retardant curing agents and a study of their effect on thermal properties of epoxy resins, J. Coat. Technol. Res. 11 (2014) 631–637.

[23] C. Hamciuc, D. Serbezeanu, I.-.D. Carja, T. Vlad-Bubulac, V.-E.; Forrat Musteata, V. Pérez, C. Guillem López, A.M. López Buendia, Effect of DOPO units and of polydimethylsiloxane segments on the properties of epoxy resins, J. Mater. Sci. 48 (2013) 8520–8529.

[24] K. Zhang, M.-.M. Shen, K. Wu, H.-.F. Liu, Y. Zhang, Comparative study on flame retardancy and thermal degradation of phosphorus- and silicon-containing epoxy resin composites, J. Polym. Res. 18 (2011) 2061–2070.

[25] S. Song, J. Ma, K. Cao, G. Chang, Y. Huang, J. Yang, Synthesis of a novel dicyclic silicon-/phosphorus hybrid and its performance on flame retardancy of epoxy resin, Polym. Degrad. Stab. 99 (2014) 43–52.

[26] Z. Li, R. Yang, Study of the synergistic effect of polyhedral oligomeric octadiphenylsulfonylsilsesquioxane and 9,10-dihydro-9-oxa-10-phosphaphenanthrene-10-oxide on flame-retarded epoxy resins, Polym. Degrad. Stab. 109 (2014) 233–239.

[27] W. Zhang, X. Li, H. Fan, R. Yang, Study on mechanism of phosphorus–silicon synergistic flame retardancy on epoxy resins, Polym. Degrad. Stab. 97 (2012) 2241–2248.

[28] X. Wang, Y. Hu, L. Song, W. Xing, H. Lu, Thermal degradation behaviors of epoxy resin/POSS hybrids and phosphorus-silicon synergism of flame retardancy, J. Polym. Sci. B Polym. Phys. 48 (2010) 693–705.

[29] Hexcel Inc Product Data Sheet RTM6. www.hexcel.com.

[30] T.J. Schuster, S. Eibl, H.-.J. Gudladt, Influence of carbon nanotubes on thermal response and reaction to fire properties of carbon fibre-reinforced plastic material, J. Compos. Mater. 52 (5) (2017) 567–579.

[31] DIN EN 60695-11-10 (2015) Prüfungen zur Beurteilung der Brandgefahr - Teil 11-10: prüfflammen - Prüfverfahren mit einer 50-W-Prüfflamme horizontal und vertikal (IEC 60695-11-10:2013).

[32] V. Babrauskas, Development of the cone calorimeter-A bench-scale heat release rate apparatus based on oxygen consumption, Fire Mater. 8 (2) (1984).

[33] ISO 5660-1,2Reaction-to-fire Tests - Heat Release, Smoke Production and Mass Loss Rate, Switzerland, 2002.

[34] B. Schartel, T.R. Hull, Development of fire-retarded materials—Interpretation of cone calorimeter data, Fire Mater. 31 (5) (2007) 327–354.

[35] DIN EN 2563:1997-03 Aerospace series- carbon fiber Reinforced plastics- unidirectional laminates; determination of apparent interlaminar shear strength.

[36] B. Perret, B. Schartel, K. Stöß, M. Ciesielski, J. Diederichs, M. Döring, J. Krämer, V. Altstädt, Novel DOPO-based flame retardants in high-performance carbon fibre epoxy composites for aviation, Eur. Polym. J. 47 (5) (2011) 1081–1089.

[37] E.D. Weil, W. Zhu, N. Patel, S.M. Mukhopadhyay, A systems approach to flame retardancy and comments on modes of action, Polym. Degrad. Stab. (54) (1996) 125–136.

[38] O. Petreus, F.N. Popescu, C.N. Cascaval, Action of some organophosphonic compounds on a diglycidyl ether-bisphenol-A epoxy resin, Die Angewandte Makromolekulare Chemie (222) (1994) 13–23.

[39] N. Rose, M. Le Bras, R. Delobel, B. Costes, Y. Henry, Thermal oxidative degradation of an epoxy resin, Polym. Degrad. Stab. 42 (3) (1993) 307–316.

[40] N. Rose, M. Le Bras, S. Bourbigot, R. Delobel, Thermal oxidative degradation of epoxy resins: evaluation of their heat resistance using invariant kinetic parameters, Polym. Degrad. Stab. 45 (1994) 387–397.

[41] D.W. McKee, C.L. Spiro, E.J. Lamby, The inhibition of graphite oxidation by phosphorus additives, Carbon 22 (3) (1984) 285–290.

[42] W. Zhang, X. Li, H. Fan, R. Yang, Study on mechanism of phosphorus-silicon synergistic flame retardancy on epoxy resins, Polym. Degrad. Stab. 97 (11) (2012) 2241–2248.